Modelling of Single Droplet Drying and Morphology Evolution using Meshfree Simulation Methods

W. Säckel*, F. Keller, U. Nieken
Institute of Chemical Process Engineering, University of Stuttgart, Germany
saeckel@icvt.uni-stuttgart.de and nieken@icvt.uni-stuttgart.de

Abstract

Spray drying is a widely used process. However, in many cases process parameters need to be evaluated empirically in order to achieve the desired product properties. In common drying models of single droplets often only radial distributions of a quantity are calculated according to effective transport parameters, which need to be fitted to experiments. The substructure and its morphology and properties inducing the transport behaviour cannot be predicted. The present contribution introduces a novel approach for single droplet drying models based on the meshfree method Smoothed Particle Hydrodynamics. By calculating the underlying physical effects on a detailed scale the morphology evolution inside the droplet shall be predicted in future. First applications to drying and a future perspective are shown.

Introduction

Spray processes offer a broad variety of applications. Especially spray drying is widely used in industrial applications. However, process parameters very often need to be derived in an empirical manner, as the evolution of a particle's morphology during drying and the underlying processes cannot be sufficiently simulated yet. Moreover, reactive spray drying processes such as spray polymerisation – though being very promising – are rarely applied due to the lack of understanding of these processes.

Common models regarding single droplets typically postulate a spherically symmetric morphology. Model equations are then set up one-dimensionally in radial direction. While the drying process and its kinetics can be simulated very efficiently, non-symmetric morphologies are not regarded and the influence of substructures is often implemented using empirical, "effective" transport parameters. Product properties like the products porosity or breaking strength can hardly be predicted with this approach. For a deeper understanding of the processes and the morphology evolution inside a droplet a detailed model, which accounts for the underlying processes, is very desirable. However, these details include pores, fractures, multiphase systems and moving interfaces inside the droplet, thus making a simulation of the process very demanding. Meshfree methods may be able to cope with these challenges. Frank and Perré [1] gave an overview on such methods with respect to single effects occurring in drying applications. Still, there hardly exists any model, which combines these effects and applies them to droplet drying. A first approach will be presented in the following.

Meshfree Methods

Meshfree methods approximate or discretise the continuum via interpolation points, usually called "particles" in this context. These particles can move independently from each other according to a Lagrangian viewpoint and represent a certain mass and other "inner variables" such as pressure, temperature etc. Particles should not be considered as hard spheres or granular masses. They are truly interpolation points. The algorithmic schemes (e.g. neighbourhood search) are related to those of molecular dynamics. However, the meshfree approximation does not adopt an atomistic view and solves the continuum laws where discrete values of single atoms are averaged out.

In computational fluid dynamics meshfree methods are not as widely used as grid-based techniques. Nevertheless they do provide some interesting features in comparison to established methods for special applications. Due to their point-based approximation meshfree methods can handle large material deformations up to the evolution of cracks in materials, which makes them popular for impact calculations. Costly remeshing procedures are not necessary. Free surfaces or interfaces in multiphase systems do not need to be detected, as different phases can be incorporated using different particle classes. Interfaces are tracked automatically with the interfacial particle movement. Therefore meshfree methods provide a promising option for the calculation of morphology evolution within a process like spray drying.

* Corresponding author: saeckel@icvt.uni-stuttgart.de

Smoothed Particle Hydrodynamics (SPH)

Lucy [2] and Gingold and Monaghan [3] (partly) independently developed the Smoothed Particle Hydrodynamics method (SPH) in 1977 for astrophysical applications. The mathematical derivation relies on interpolation theory. An estimated value of a quantity f can be calculated via an integral approximation [2][3][4]

$$\langle f(\mathbf{r})\rangle = \int f(\mathbf{r}')\delta(\mathbf{r}-\mathbf{r}')d\mathbf{r}'. \tag{1}$$

δ is the delta function and d**r**' a differential volume element. In the context of SPH f may be a physical quantity like the density, pressure etc. The delta function can be approximated using

$$\delta(\mathbf{r}-\mathbf{r}') = \lim_{h\to 0} W(\mathbf{r}-\mathbf{r}',h) \tag{2}$$

with a kernel function W, which therefore needs to meet several requirements. With the kernel's length scale h (typically called the smoothing length) tending to zero the kernel function needs to approach the delta function. It must be symmetric and its integral must be normalised to one. As spatial derivatives of the calculated values will also be approximated via the kernel function, it needs to be continuously differentiable at least once. With a kernel function of finite length scale h equation (1) can be rewritten as [4]

$$\langle f(\mathbf{r})\rangle = \int f(\mathbf{r}')W(\mathbf{r}-\mathbf{r}',h)d\mathbf{r}' + O(h^2). \tag{3}$$

For a calculation with a discrete number of points the integral is changed to a summation and the second order error term is omitted. The infinitesimal volume element d**r'** becomes a finite volume, usually expressed via the quotient of mass and density:

$$f_i = \sum_j \frac{m_j}{\rho_j} f(\mathbf{r}_j) W_{ij}(h). \tag{4}$$

The value f for a particle i is then expressed using the values of all particles j (including i itself) multiplied with the kernel function $W_{ij}(h)$ evaluated for the distance between the particles i and j taking into account the smoothing length h. For reasons of computational efficiency typical kernel functions have a compact support beyond which they become zero, so that only a small neighbourhood of particles j needs to be regarded. Cut-off radii usually lie within a distance of two or three times h (also depending on the formulation of the kernel function with respect to h). The first spatial derivative of f can be evaluated via [4]

$$\nabla f_i = \sum_j \frac{m_j}{\rho_j} f_j \nabla_i W_{ij}(h), \tag{5}$$

the kernel's gradient being expressed with its derivative and the unit vector $\mathbf{e_{ij}}$ between particles i and j [5]:

$$\nabla_i W_{ij}(h) = \mathbf{e_{ij}} \frac{dW_{ij}(h)}{dr}. \tag{6}$$

$\mathbf{e_{ij}}$ is the unit vector between particles i and j [5]. A second derivative of a quantity f could be formulated by differentiating the kernel twice, however this approach has proven to be very sensitive regarding particle disorder [4]. Thus a formulation like the following is usually used, which applies a sort of finite difference scheme for differentiating a second time:

$$(\nabla^2 f)_i = 2\sum_j \frac{m_j}{\rho_j} \frac{f_i - f_j}{r_{ij}} \frac{dW_{ij}(h)}{dr}. \tag{7}$$

The value r_{ij} denotes the absolute value of the distance between both position vectors $\mathbf{r_i}$ and $\mathbf{r_j}$.

Typical kernels amongst others are the Gaussian kernel or spline kernels [4]. Though Gaussian functions provide a nice approximation they do not become zero at a certain cut-off radius. Therefore spline kernels are used in very many simulations. The cubic spline used in the simulations presented here is calculated by

$$W(q) = \begin{cases} a\left[(2-q)^3 - 4(1-q)^3\right] & 0 \le q \le 1 \\ a\left[(2-q)^3\right] & 1 \le q \le 2 \\ 0 & q > 2 \end{cases}, \qquad q = \frac{|\mathbf{r_i} - \mathbf{r_j}|}{h}. \tag{8}$$

As mentioned before the integral of the kernel function needs to be unity in order to provide a correct approximation of the delta function. Thus the prefactor a in equation (8) depends on the dimensions of the problem. It is replaced by $1/(4\pi h^3)$ for a three-dimensional calculation and by $15/(14\pi h^2)$ in two dimensions [4].

Using equation (5) for example the density of a particle can be computed via

$$\rho_i = \sum_j m_j W_{ij}(h). \tag{9}$$

Time integration is usually performed using explicit methods. An implicit formulation, although possible in principle, is hard to implement efficiently as the neighbourhood of particles and therefore their connectivity can change between integration steps (and therefore between single iterations of an implicit solver).

Model Equations

Contrary to most literature models on single droplet drying the SPH model will be written in Cartesian coordinates, as there are very few applications using spherical coordinates in SPH and the model shall account for arbitrary structures anyway. Typical drying models (e.g. [6][7]) calculate radial distributions of the droplet's temperature and the mass fraction of a solvent. Heat and mass transfer to the surrounding gas are implemented using Nusselt and Sherwood correlations. An SPH formulation for the heat conduction equation

$$\frac{\partial T}{\partial t} = \frac{1}{c_p \rho} \nabla(\lambda \nabla T) \tag{10}$$

can be found in [8]

$$\frac{dT_i}{dt} = \frac{2}{c_{p,i}} \sum_j \frac{m_j}{\rho_i \rho_j} \frac{2\lambda_i \lambda_j}{\lambda_i + \lambda_j} \frac{T_i - T_j}{r_{ij}} \frac{dW_{ij}(h)}{dr}, \tag{11}$$

where the change of a particles temperature T is calculated assuming the heat capacity c_p not being a function of temperature and using the approach of equation (7). The average heat conduction coefficient λ is calculated via a harmonic mean, as the heat transferred between two points will become zero when one of both points is a perfect isolator with λ=0. Diffusion according to Fick's second law can be formulated analogously.

However, the implementation of boundary conditions in SPH can be cumbersome. Hardly any literature exists on Nusselt and Sherwood correlations in SPH formulations, which are more complicated compared to a common grid-based model using algebraic boundary conditions [9]. A flux per unit area needs to be applied to surface particles with a particular surface area, which can only be calculated directly for simple geometries. A solution was found using the CSF approach of Brackbill et al [10], which was originally derived for the implementation of surface tension, a phenomenon that also only occurs at an interfacial surface. Brackbill transformed the infinitesimal small interface area into a smooth interface volume expanding into both adjoining phases. A so called "colour function" c which is different on both sides of the interface and changes smoothly within the interfacial volume gives a transformation between an area based value f_A and its volume-based pendant f_V:

$$f_V = f_A \cdot \frac{\nabla c}{[c]}. \tag{12}$$

[c] denotes the total jump of c over the interface thus normalising the transformation. This calculation needs to be done for all nodes within the interface volume. Morris [11] translated the CSF model into SPH equations:

$$\frac{\nabla c}{[c]} = \frac{1}{[c]} \sum_j \frac{m_j}{\rho_j} c_j \nabla W_{ij}(h). \tag{13}$$

Thus heat transfer at the liquid-gas interface can be expressed in SPH using

$$\left.\frac{\partial T_i}{\partial t}\right|_{Nu} = -\frac{\nabla c}{[c]} \frac{\alpha}{c_{p,i} \rho_i} (T_i - T_\infty) \tag{14}$$

with α being the heat transfer coefficient [9]. Analogously mass transfer may be formulated according to

$$\frac{dm_i}{dt} = -V_i MW_l \frac{\nabla c}{[c]} \frac{\beta}{\Re T} (p_{v,i} - p_{v,\infty}). \tag{15}$$

V_i is the particle volume, MW_l the molar mass of the evaporating liquid, β the mass transfer coefficient and R the universal gas constant. A surface particle will lose mass until it reaches zero and will then be converted into a gas particle. The vapour pressure of liquid at the surface p_v can be calculated using e. g. Antoine's law, as long as liquid SPH particles consist of pure solvent, which is the case in this study. The vapour pressure of a mixture in a future drying model (e. g. reactive drying) needs to be calculated using an appropriate model for vapour-liquid equilibrium at the phase boundary like Raoult's law.

When a crust formation occurs during drying, the transport limitation through the pores needs to be regarded. A detailed model should resolve the crust and calculate mass transport through the pores directly. Therefore the gas phase inside the pores needs to be regarded. Diffusion of vapour can be modelled using Fick's diffusion expressed for the vapour pressure p_v with the diffusion coefficient D:

$$\frac{dp_{v,i}}{dt} = 2 \sum_j \frac{m_j}{\rho_j} \frac{2 D_i D_j}{D_i + D_j} \frac{p_{v,i} - p_{v,j}}{r_{ij}} \frac{dW_{ij}(h)}{dr}. \tag{16}$$

Applying equation (16) to surface liquid particles with p_v set to the saturation pressure of the liquid the mass loss of such a particle can be expressed via

$$\frac{dm_i}{dt} = -\frac{V_i MW_l}{\Re T} \frac{dp_{v,i}}{dt}. \tag{17}$$

For particle movement the Euler acceleration equation (Lagrangian formulation)

$$\frac{D\mathbf{v}}{Dt} = -\frac{\nabla p}{\rho} + \mathbf{f} = -\nabla\left(\frac{p}{\rho}\right) - \frac{p}{\rho^2}\nabla\rho + \mathbf{f} \tag{18}$$

can be transformed using equation (5) and the second part of equation (18) to the SPH expression [4]

$$\frac{d\mathbf{v}_i}{dt} = -\sum_j m_j \left(\frac{p_i}{\rho_i^2} + \frac{p_j}{\rho_j^2}\right) \nabla_i W_{ij}(h) + \mathbf{f}_i. \tag{19}$$

The vector **f** denotes external forces, **v** is the velocity and p the pressure. In Navier-Stokes equations viscous forces add up to equations (18) and (19). For Newtonian fluids the term

$$\left(\frac{\mu}{\rho}\nabla^2\mathbf{v}\right)_i = \sum_j \frac{4m_j(\mu_i + \mu_j)\mathbf{r_{ij}}\nabla_i W_{ij}(h)}{(\rho_i + \rho_j)^2\left(r_{ij}^2 + \eta^2\right)}\left(\mathbf{v_i} - \mathbf{v_j}\right) \tag{20}$$

needs to be regarded [12], with μ being the dynamic viscosity. Non-Newtonian rheologies can be implemented applying the SPH formulations to the respective formulae [12][13].

Pressure calculation in SPH can be performed using an equation of state. This approach is not only implemented for gases, but also very often for incompressible liquids. A very stiff equation, usually the Tait equation

$$p = \frac{\rho_0 c_s}{\gamma}\left(\left(\frac{\rho}{\rho_0}\right)^{\gamma} - 1\right), \tag{21}$$

is applied with the adiabatic exponent γ typically chosen to 7 and the speed of sound c_s such that density fluctuations stay within the range of 1 % [4]. However, in the present contribution a predictor-corrector projection scheme is applied for the liquid phase, where in a first step intermediate particle positions are calculated and then – according to the continuity equation – a pressure Poisson equation is solved such that in the correction step the movement due to the pressure ensures incompressibility. The course of action is similar to well-known approaches like SIMPLE and explained in detail in [12] and [13]. Moving solids within the liquid phase are treated as a liquid in a first step and then corrected using a rigid body approach proposed by Koshizuka and Shao [14][15], which ensures constant particle distances to the centre of gravity of the respective body and conserves its linear and angular momentum.

As transport in pores is diffusion controlled, gas dynamics do not need to be modelled in detail. Still the gas particles need to arrange themselves depending on the positions of fluid surface and a reasonably good particle distribution for the calculation of diffusive vapour transport is required, Thus for reasons of simplicity the movement of gas particles is modelled using the weakly incompressible technique with liquids and solids being solid boundaries. Alternatively, the gas phase also could be modelled in an additional predictor-corrector step [16], which is an option for future models.

Surface tension forces can be implemented using the well-known CSF method [10][11]. This course of action was undertaken in a preliminary study of the drying model. However, the modelling of wetting and contact angles in SPH is not solved sufficiently yet, so that many groups use an alternative approach based on pairwise interactions of interpolation points. By applying different forces between different particle classes a wetting behaviour can be parameterised. Although this method is very intuitive, its drawback is the parameterisation, which needs to be undertaken carefully and does not generally converge for different length scales [17]. Current research in our group is concerned with a future implementation directly connected to continuum laws of surface tension and wetting behaviour. However, a force-based approach is still applied in the drying model. The formula is related to the one proposed by Tartakovsky and Meakin [18], enhanced by a strong repulsive force for particles going below the particle spacing/length scale l_0 and parameterised with a factor s_{ij}:

$$\mathbf{f} = k \cdot s_{ij} \cos\left(\pi \frac{r_{ij} - 0.5\left(r_{cut-off} + l_0\right)}{r_{cut-off} - l_0}\right)\mathbf{e_{ij}}, \qquad k = \begin{cases} 1 & r_{ij} \geq l_0 \\ -10 & r_{ij} < l_0 \end{cases}. \tag{22}$$

The SPH method is well suited for parallelisation, which has been undertaken in many astrophysical SPH codes. However our current code is not completely parallelised yet, so that the presented results have been calculated in a serial version, not allowing for high particle numbers. All simulations were undertaken using a cut-off radius of 3.1 times the particle spacing l_0. Although the cut-off can be kept at about $2\,l_0$ in many applications, simulations, in which surface tension plays a role or a CSF approach is applied, require a larger number of neighbouring particles.

Numerical Results

As has already been pointed out, the formulation of Nusselt and Sherwood boundaries in SPH is cumbersome. In order to provide a proof of concept a first implementation regarded the evaporation of pure liquid. The temperature distribution inside the droplet and heat and mass transfer to surrounding gas were taken into account. A three-dimensional SPH formulation was applied to a cone-shaped droplet cut-out and compared with a

respective one-dimensional, spherically symmetric formulation using finite differences. The results can be seen in Figure 1. SPH results agree well with the mesh-based calculation. Heat and mass transfer can be calculated accurately for different geometries using the CSF approach, as the left and middle frames show calculations for droplets whereas the right frame contains results for a flat surface. For droplet drying both the heat up time of 3 s for the conditions in the left frame and the d²-law in the middle frame are calculated correctly. Deviations occur at small radii, when the droplet radius lies in the same length scale as the interpolation points' size.

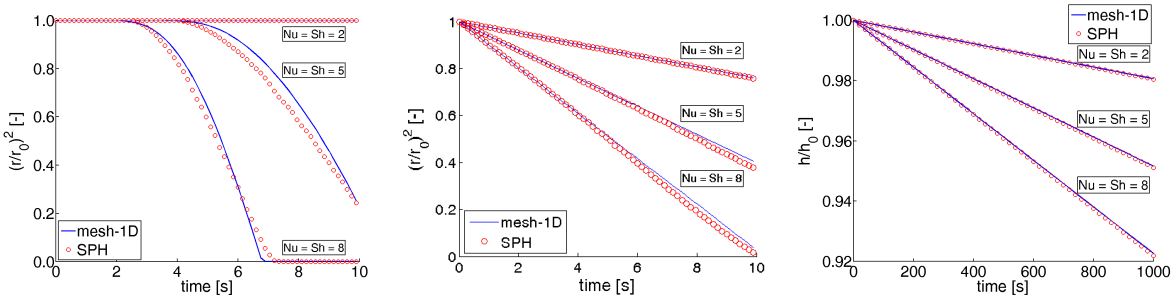

Figure 1 Simulation of the evaporation of a pure liquid at a relative humidity of 50 %; geometries: droplet (l/m), semi-infinite basin (r); T^g = 100 °C, T^l_{start} = 40 °C (l), $T^g = T^l_{start}$ = 60 °C (m/r)

For reasons of simplicity in this first prove of concept, both liquid and gas particles were fixed. The following study shows an enhanced, two-dimensional model, where particle motion and additionally suspended solids are regarded. The motion of the liquid phase (water) is modelled using the predictor-corrector scheme. Suspended solids are implemented by Shao's rigid body approach and have the same density as the liquid, so that buoyancy effects don't affect the solution. However, the model would be able to handle different densities, if the ratio was not too large. The gas phase is omitted here, as the CSF approach can be applied to a free liquid surface in SPH, too, to simulate the drying behaviour. The interactive force is parameterised with a prefactor s being 50 times the particle spacing $l_0 = 0.25 \cdot 10^{-3}$ m for particles of the same kind. In order to keep simulation times low the drying effect was scaled in such a way that five layers of liquid particles would evaporate on a flat surface within a second's time. This scaling can be undertaken as long as it does not affect the simulation results significantly. As can be seen in the following calculations, particles arrange themselves to a quasi equilibrium state very quickly due to the small time-scale of surface tension and wetting. An acceleration of the drying process, if not undertaken too rapidly, does rarely affect this equilibrium and should therefore only have a small effect on the result.

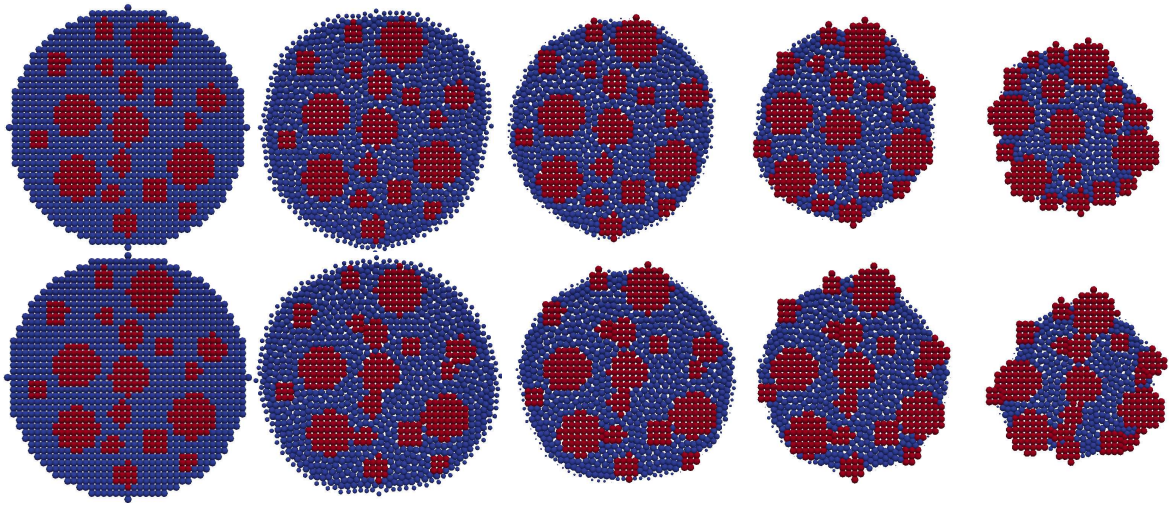

Figure 2 Drying of a suspension of large solids at times 0, 75, 500, 1000 and 2000 ms. In the first row, the interaction between liquid and solids is strong, in the second row weak.

In Figure 2 the first shows a simulation where the interaction between solid and liquid particles was set to 1.2 times stronger than forces between particles of the same type. The red points represent solid particles, the blue ones water. In less than 75 ms particles rearrange themselves. This effect is caused by the initial setup of particles on a cubic lattice, which is not set to an energetic optimum regarding inter-particle forces. Also the droplet is a bit deformed because of the inter-particle forces, an effect, which should vanish when calculating at higher resolutions. When the drying process proceeds solids stay wetted first due to the higher liquid-solid attraction. After some time the solid fraction at the surface is so high, that only very small pores remain between the solids. The drying rate decreases strongly. A further calculation with this approach would show the very slow depletion of pores, taking also a very long computation time. The product in the end would be rather dense.

However the CSF drying approach was intended to implement drying rates based on Sherwood correlations and is not applicable to the transport within pores in the second drying period.

In the second row of Figure 2 the forces between different phases were set to 0.9 times the interaction between particles of the same kind, thus leading to relatively stronger liquid-liquid and solid-solid interactions. A strong attraction between solids could for instance model the effect of a binder in a suspension. Again, particles arrange to an equilibrium rapidly. Simultaneously, the solids begin to cluster. When there is only a single layer of liquid particles between two solids these liquids are squeezed out due to the smaller attraction between different phases. Still, liquid particles can be "trapped" between two solids for geometrical reasons. With the liquid surface drawing back the clustering process goes on leading to a development of pores filled with liquid. In the end a rather porous product is achieved. For the same reason as before the simulation was stopped with the beginning of the second drying period. However, the pores in this simulation are significantly larger than in the one.

In the simulation shown by Figure 3 the suspended solids were smaller. It can be seen, that the principle effects stay the same. In the first case the liquid-solid interaction was increased with a factor 1.5 leading to single particles, which are fully wetted for a long time, whereas a weaker interaction of factor 0.9 causes clustering of solids in the second phase. However as the smaller solids are more mobile this clustering takes place in a different manner. After a relatively short time the droplet surface is partly covered with a solid crust, leaving large liquid reservoirs below. Still, the size of the remaining pores at the surface is comparably large.

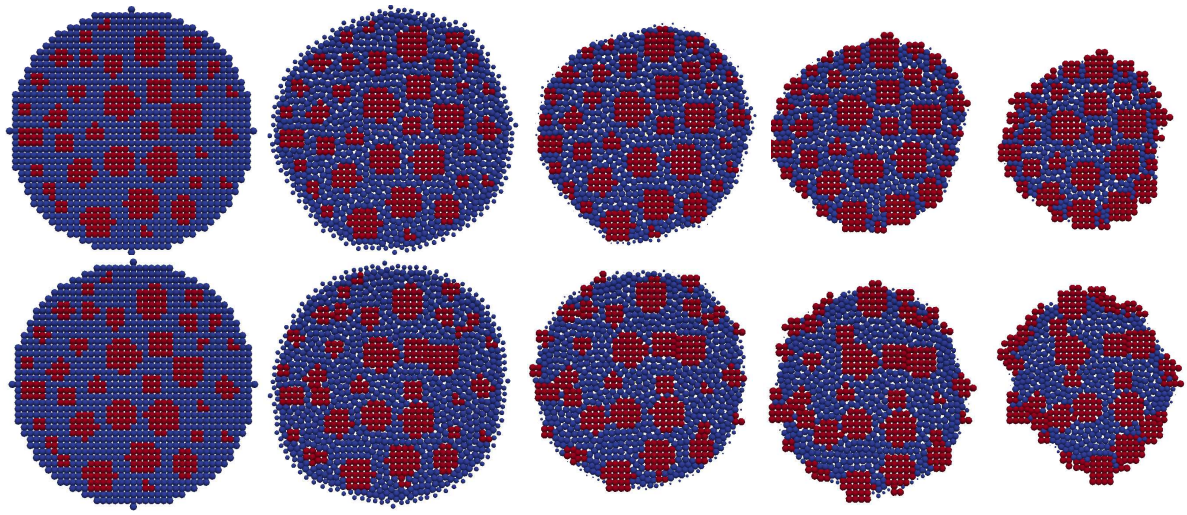

Figure 3 Drying of a suspension of small solids at times 0, 75, 500, 1000 and 2000 ms.
In the first row, the interaction between liquid and solids is strong, in the second row weak.

Simulation times for this model are relatively large. A simulation of a droplet containing initially 1257 particles took about 16 hours for one second's time in the drying process, ran on one core of a Core i7 workstation. The most time-consuming step is the solution of the Poisson pressure equation. Profiling indicates that the present solver might not be an optimal choice, so that simulation times could be significantly smaller. Still parallelisation is a major task in our model development.

The simulations presented before showed a formation of pores. In order to model the second drying phase, where diffusive transport through a porous crust is dominant, the next example implements the drying process inside a porous structure. Solids have fixed positions. The bottom, the left and the right of the domain are limited by fixed liquid particles, whereas the upper pore region is represented by gas particles with fixed vapour pressures and positions. Mass transfer of liquid surface particles to the gas phase is modelled according to equations (16) and (17) and was scaled again in order to keep simulation times moderate. Evaporating liquid particles are transformed into gas points, which arrange themselves between the liquid surface and the upper fixed border according to the weakly incompressible approach.

Figure 4 shows results at different times. Gas is represented by small particles with the colour indicating the vapour pressure. Liquid particles are blue, solids red. Comparing the liquid surface's position at different times the drying rate decelerates throughout the drying process, as it should be expected for pores/the diffusion pathway getting longer. Due to wetting effects the liquid sticks to the solids and menisci are formed at the surface. The pores on the left quarter of the domain are larger than the other ones and therefore evaporation takes place faster there as can be seen in frames 3 and 4. Moreover, the distribution of gas particles is best if the pores are not too narrow. On the contrary the gas particles, which reside in the small pores between the three big solids in the upper middle, are distributed rather unevenly. Still the example shows, that the proposed approach is able to model the second drying phase.

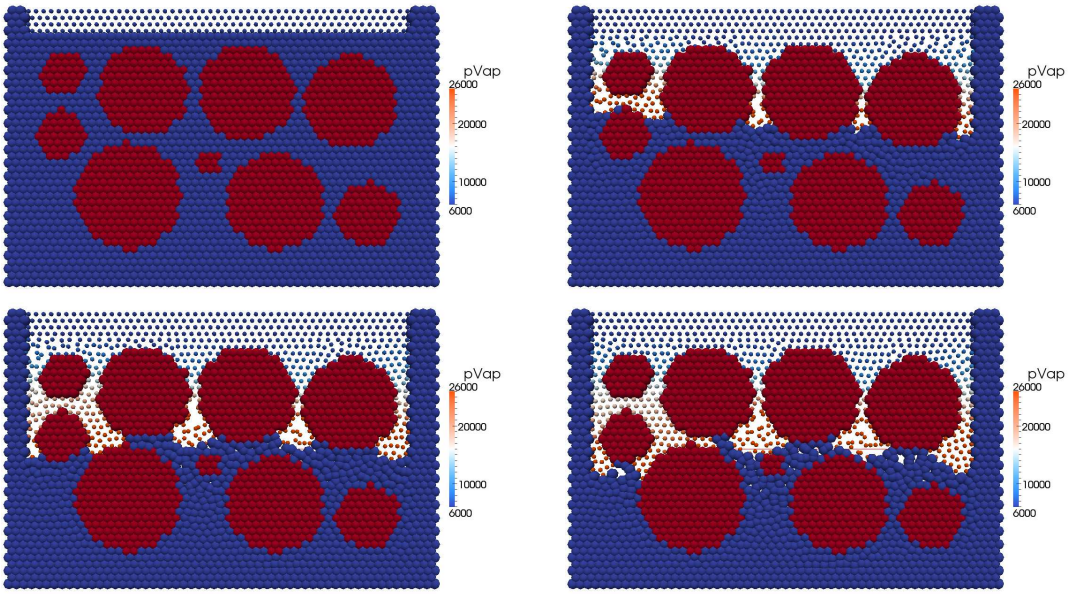

Figure 4 Diffusive vapour transport inside a porous layer

Discussion

The simulation of morphology evolution is challenging and the underlying processes, which need to be regarded in single droplet drying, are numerous. The SPH approach has proven to be capable of simulating both the drying process as well as the morphology determining physics. The results of established grid-based models can be reproduced. By applying particle motion, surface tension and wetting an insight into a droplet during the drying process can be undertaken. A variation of physical properties leads to different structures of the product, thus underlining the ability of the method for the simulation of morphology evolution. The second drying phase can be modelled and shall be applied to the droplet in a future model. Still, the approach is relatively new and several challenges regarding the method or the process itself need to be addressed. Although the results are reasonable, the particle number was relatively low. In the near future, simulations shall be undertaken at higher resolutions. Additionally, the implementation of surface tension and wetting though representing a qualitatively correct behaviour should be revised. As stated out before, a technique based on continuum laws, surface tension coefficients and contact angles is subject to current research.

Another challenge concerns the SPH method. Deficiencies can arise when the neighbourhood of a particle is only partly filled (e.g. at surfaces) and consequently the kernel function is not normalised to one anymore. This question has been widely addressed in literature and there exist several renormalisation approaches (for instance see [19], [20] and [21]), which have been successfully tested in a related project. An implementation of these routines into the drying model is possible and shall be one of the next steps in our model development.

A general question regarding simulations on a detailed length scale comprises in fluid dynamics as – for instance using CFL criteria – the maximum time steps decrease proportional with a smaller length scale/finer resolution, while the number of particles in the simulation rapidly increases, depending on the dimensionality of the problem. Additionally capillary forces become large compared to the particle mass thus leading to high accelerations. Evaporation, however, is a fairly slow process, thus requiring long simulation times. This is not a special drawback of the SPH approach as grid-based methods encounter the same challenges. Still, this fact needs to be taken into account when thinking about possible model resolutions and the focus of future research.

Outlook

Though the meshfree approach could be applied to very many possible questions in drying applications in principle, research should still be focused on a few areas in the near future. First of all, the droplet drying model should be further developed. The second drying period with diffusive transport through the pores shall be implemented into the droplet model as shown for the porous structure. Surface tension and wetting should be based on continuum laws rather than on a parameterised inter-particle force or at least both formulation and parameterisation of this force need to be validated intensely. Also the consequences, when physical effects like evaporation are scaled, should be further investigated in order to keep scaling within reasonable limits and to achieve tolerable simulation times.

The second main subject in future research should address simulations of small, representative volumes of the whole droplet in order to avoid particle numbers going too high. Although the idea of simulating a whole droplet on a detailed scale during the whole process is appealing, simulations on a very small scale are still com-

putationally very expensive. Still many effects can be simulated using relatively small representative equivalent volumes. Effective transport parameters for a porous crust could then be obtained by SPH calculations as well as crust properties like pore sizes and their distributions and be applied to a grid-based 1D model of the droplet. Like in other research areas multi-scale simulations are a very promising alternative to being either too detailed or too coarse. Still, a reliable identification of representative volumes and a reasonable coupling of different scales are inevitable and therefore require further research.

An application of the method to reactive drying processes is possible and shall be undertaken regarding spray polymerisation in a future model. Especially for this application the current approach is very promising, as previous research regarding the simulation of reaction induced morphology evolution has already shown the potential of the SPH method [13].

Acknowledgements

This project is part of the priority program 1423 “Prozess Spray” of the Deutsche Forschungsgemeinschaft. We kindly thank the DFG for their financial support.

References

[1] Frank, X., Perré, P., *Drying Technology* 28: 932–943 (2010).
[2] Lucy, L.B., *Astronomical Journal* 82: 1013–1024 (1977).
[3] Gingold, R.A., Monaghan, J.J., *Monthly Notices of the Royal Astronomical Society* 181: 375–389 (1977).
[4] Monaghan, J.J., *Reports on Progress in Physics* 68: 1703–1759 (2005).
[5] Rosswog, S., *New Astronomy Reviews* 53: 78–104 (2009).
[6] Sloth, J., Kiil, S., Jensen, A. D., Andersen, S. K., Jørgensen, K., Schiffter, H., Lee, G., *Chemical Engineering Science* 61: 2701–2709 (2006).
[7] Mezhericher, M., Levy, A., Borde, I., *Drying Technology* 27: 870–877 (2009).
[8] Cleary, P.W., *Applied Mathematical Modelling* 22: 981–993 (1998).
[9] Säckel, W., Keller, F., Nieken, U., *Proceedings 9. Workshop über Sprays, Techniken der Fluidzerstäubung und Untersuchungen von Sprühvorgängen*, Heidelberg, editors: Gutheil, E., Fritsching, U., http://elib.suub.uni-bremen.de/ip/docs/00010639.pdf (2010).
[10] Brackbill, J.U., Kothe, D.B. and Zemach, C., *Journal of Computational Physics*. 100: 335–354 (1992).
[11] Morris, J.P., *International Journal for Numerical Methods in Fluids* 33: 333–353 (2000).
[12] Shao, S., Lo, E. Y. M., *Advances in Water Resources* 26: 787–800 (2003).
[13] Keller, F., Nieken, U., *Meshfree Methods for Partial Differential Equations V*, New York: Springer, editors: Griebel, M., Schweitzer, M. A., 2010.
[14] Koshizuka, S., Nobe, A., Oka, Y., *International Journal for Numerical Methods in Fluids* 26: 751–769 (1998).
[15] Shao, S., *International Journal for Numerical Methods in Fluids* 59: 91–115 (2009).
[16] Khayyer, A., Gotoh, H., *Coastal Engineering* 56: 419–440 (2009).
[17] Adami, S., Hu, X., Adams, N. A., *Journal of Computational Physics* 229: 5011–5021 (2010).
[18] Tartakovsky, A. M., Meakin, P., *Phys. Rev. E* 72: 26301 (2005).
[19] Randles, P. W., Libersky, L. D., *Computer Methods in Applied Mechanics and Engineering* 139: 375–408 (1996).
[20] Bonet, J., Lok, T. S., *Computer Methods in Applied Mechanics and Engineering* 180: 97–115 (1999).
[21] Grenier, N., Antuono, M., Colagrossi, A., Le Touzé, D., Alessandrini, B., *Journal of Computational Physics* 228: 8380–8393 (2009).